

# Unsupervised Place Recognition with Deep Embedding Learning over Radar Videos

Matthew Gadd<sup>†</sup>, Daniele De Martini<sup>†</sup>, and Paul Newman

Oxford Robotics Institute, Dept. Engineering Science, University of Oxford, UK.

{mattgadd, danielle, pnewman}@robots.ox.ac.uk

**Abstract**—We learn, in an unsupervised way, an embedding from sequences of radar images that is suitable for solving place recognition problem using complex radar data. We experiment on 280 km of data and show performance exceeding state-of-the-art supervised approaches, localising correctly 98.38 % of the time when using just the nearest database candidate.

**Index Terms**—Radar, Place Recognition, Deep Learning, Unsupervised Learning, Autonomous Vehicles

## I. INTRODUCTION

For autonomous vehicles to drive safely at speed, in inclement weather, or in wide-open spaces, very robust sensing is required. Thus, the interest in scanning FMCW radar for place recognition and localisation. As more datasets featuring this modality become available, unsupervised techniques will allow us to learn from copious unlabelled measurements. This paper presents initial results in that vein.

## II. RELATED WORK

Kim *et al* [1] show that radar can outperform LiDAR in place recognition using a non-learned rotationally-invariant ring-key descriptor. Săftescu *et al* [2] present the first supervised deep approach, adapting CNNs for equivariance and invariance to azimuthal perturbations. Barnes and Posner [3] learn keypoints which are useful for motion estimation and localisation simultaneously. Gadd *et al* [4] leverage rotationally-invariant representations in a sequence-based localisation system. De Martini *et al* [5] fine-tune the results from the embedding space with pointcloud registration techniques. Wang *et al* learn metric localisation directly along with self-attention [6].

## III. METHOD

Our method is illustrated in Fig. 1. We adapt [7], which ensures that features of distinct instances (originally, camera images) are separated (right, arrow line between orange and blue) while features of an augmented instance are invariant (right, back-arrow line between orange and red). Our *contributions* are the sampling *as well as* augmentation strategies (top) most apposite to constrain the learning of these features for this sensor modality and the place recognition task. Here, in constructing batches of instances and their augmentations (left), we:

- 1) sample an instance randomly (orange),
- 2) pin the pre-augmented instance at 2 sec later (red),
- 3) augment either 1 or 2 (c.f. Sec. IV, vR and vT) by spinning (red,  $\circlearrowleft$ ),
- 4) pin *another* instance at 6 sec later (blue),
- 5) spin its augmentation from 2 seconds before (green,  $\circlearrowleft$ ).

<sup>†</sup> Equal contribution. This work was supported by the Assuring Autonomy International Programme, a partnership between Lloyd's Register Foundation and the University of York.

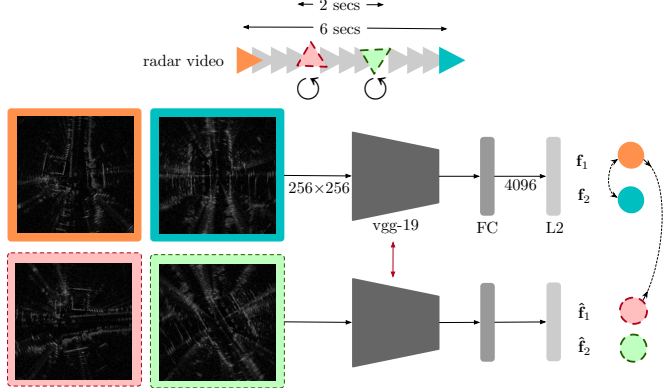


Fig. 1: Overview of our network architecture and the training procedure more generally – described in Sec. III.

Secs. IV and V prove the effectiveness of each step. Briefly, however, consider the following rationale. In step 2 we ensure that real data is presented to the network, rather than synthetic augmentations which would anyway be prohibitively difficult to simulate for radar sensor artefacts. This step also presents the network with some translational invariance, along the route driven. In step 3 we ensure rotational invariance. In step 4 we are mitigating the (already quite small but non-zero) chance that batches may simultaneously hold instances which are in fact nearby, although randomly sampled. The combination of steps 4 and 5 prepare this “true negative” as just another perturbed radar scan as per steps 1, 2, and 3, but which usefully constrains the learning in this way.

For completeness, we note that we use the VGG-19 feature extractor [8]. We train each variant for 10 epochs, using a learning rate of 3e-4, batch size of 12. Images are presented to the network in Cartesian format with dimensions  $256 \times 256$  where the side-length of each pixel represents 0.5 m.

## IV. EXPERIMENTAL SETUP

We evaluate our method in training and testing across urban data collected in the *Oxford Radar RobotCar Dataset* [9]. Train-test splits are as per [2], testing on hidden data featuring backwards traversals, vegetation, and ambiguous urban canyons. We do, however, train on most data available from [3] (barring anything from the test split) – totalling 30 forays, or about 280 km of driving. This is a similar quantity of training data as reported in [3].

We examine the performance gain available from:

- vR or “spin augmenting”: steps 1 and 3 (spinning the instance from step 1),
- vT or “video sampling”: steps 1 and 2 (no spinning),
- vTR or “video sampling and spin augmenting”: steps 1, 2, and 3, and finally

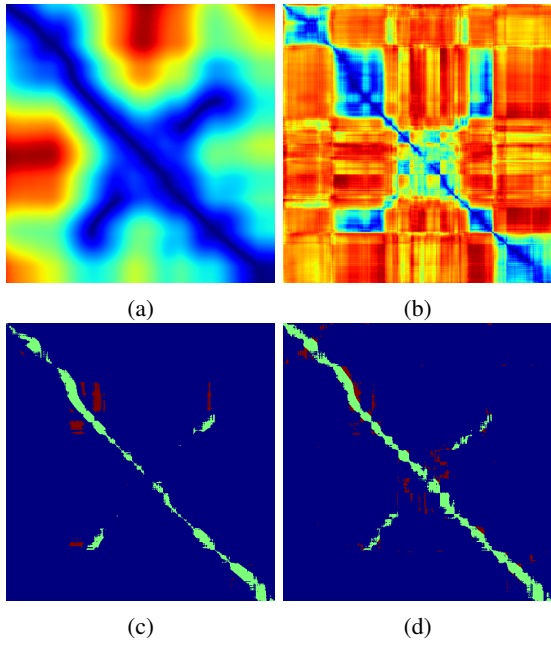


Fig. 2: (a) Ground truth matrix, (b) Distance matrix for embeddings learned by our top-performing model, vTR2, (c) match matrix for  $\text{Recall}@P=80\%$ , (d) match matrix for  $\text{Recall}@N=25$ . In (c) and (d), true positives are shown green while false positives are shown red.

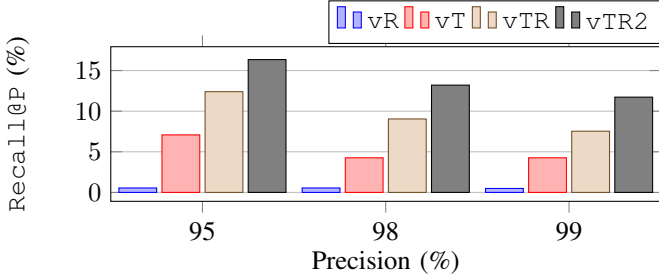


Fig. 3: Recall@P metrics, as per [2].

- vTR2: steps 1, 2, 3, 4, and 5, which we refer to as “video sampling and spin augmenting with batch pairing”.

Note the baseline of [7], entails augmenting *only* the instance itself, closest in spirit to vR.

For performance assessment, we employ both  $\text{Recall}@P$  – where predicted positives are within in a varying embedding distance threshold of the query – and  $\text{Recall}@N$  – where a query is considered correctly localised if *at least one* database candidate is close in space as measured by GPS/INS. Note that the latter is a more lenient measure of performance and that we employ no pose refinement to boost results, as in [1], [5]. We specifically impose for the first metric (Fig. 3) boundaries of 25 m and 50 m, inside of which predicted matches are considered true positives, outside of which false positives, as per [2]. The second metric (Fig. 4) supports only a single boundary, which we set to 25 m, the more difficult of the two.

## V. RESULTS

Fig. 3 shows the  $\text{Recall}@P$  metrics. We achieve from 11.72 % up to as much as 16.34 % recall for precisions of 99 % to 95 %. This is compared to 4.26 % to 7.08 % for the baseline,

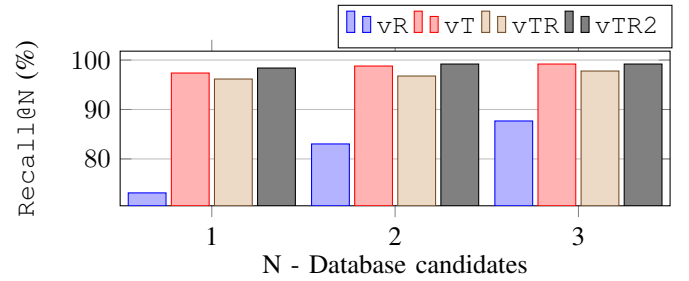


Fig. 4: Recall@N metrics, as per [9].

vR. This corresponds to  $F_1$ ,  $F_2$ , and  $F_{0.5}$  scores of 0.60, 0.55, and 0.63, respectively. Here, we have outperformed the supervised [2], where on this same test split the corresponding scores were reported as 0.53, 0.48, and 0.60.

Fig. 4 shows the Recall@N metrics. Here, we notice when only using 1 database candidate, we correctly localise 98.38 % of the time (vTR2) as compared to 73.13 % for the baseline, vR. This is also superior to the results reported in [3], approximately 97 %.

Note the fidelity of the embedding space for vTR2, Fig. 2(b), and the ground truth matrix, Fig. 2(a). Differently to Figs. 3 and 4, Fig. 2(c) shows the true and false positives for  $\text{Recall}@P=80\%$ . Fig. 2(d) shows such for  $\text{Recall}@N=25$ , similarly to [1], [9]. In both, we consider it reasonable to expect a downstream process to disambiguate *some* false matches in order to retain various types of loop closure. We see that rotational invariance is well understood by the network trained as we propose.

## VI. CONCLUSION

We have presented our initial findings for applying unsupervised learning to radar place recognition. In doing so, we outperform two previously published methods which are candidates for the current state-of-the-art, showing the great promise of unsupervised techniques in this area.

## REFERENCES

- [1] G. Kim, Y. S. Park, Y. Cho, J. Jeong, and A. Kim, “Mulran: Multimodal range dataset for urban place recognition,” in *International Conference on Robotics and Automation*, 2020.
- [2] S. Săftescu, M. Gadd, D. De Martini, D. Barnes, and P. Newman, “Kidnapped Radar: Topological Radar Localisation using Rotationally-Invariant Metric Learning,” *arXiv preprint arXiv:2001.09438*, 2020.
- [3] D. Barnes and I. Posner, “Under the Radar: Learning to Predict Robust Keypoints for Odometry Estimation and Metric Localisation in Radar,” *arXiv preprint arXiv:2001.10789*, 2020.
- [4] M. Gadd, D. De Martini, and P. Newman, “Look Around You: Sequence-based Radar Place Recognition with Learned Rotational Invariance,” *arXiv preprint arXiv:2003.04699*, 2020.
- [5] D. De Martini, M. Gadd, and P. Newman, “kRadar++: Coarse-to-fine FMCW Scanning Radar Localisation,” *Sensors*, vol. 20, no. 21, p. 6002, 2020.
- [6] W. Wang, P. P. de Gusmo, B. Yang, A. Markham, and N. Trigoni, “RadarLoc: Learning to Relocalize in FMCW Radar,” *arXiv preprint arXiv:2103.11562*, 2021.
- [7] M. Ye, X. Zhang, P. C. Yuen, and S.-F. Chang, “Unsupervised Embedding Learning via Invariant and Spreading Instance Feature,” *arXiv preprint arXiv:1904.03436*, 2019.
- [8] K. Simonyan and A. Zisserman, “Very deep convolutional networks for large-scale image recognition,” *arXiv preprint arXiv:1409.1556*, 2014.
- [9] D. Barnes, M. Gadd, P. Murcutt, P. Newman, and I. Posner, “The Oxford Radar RobotCar Dataset: A Radar Extension to the Oxford RobotCar Dataset,” *arXiv preprint arXiv:1909.01300*, 2019.